SEU Induced by Pions in Memories From Different Generations

S. Duzellier, D. Falguère, M. Tverskoy, E. Ivanov, R. Dufayel, and M.-C. Calvet

***Abstract*—This paper presents single-event upset cross-sections obtained with pions for a set of SRAMs/DRAMs from different generations. The experimental results show that pions are not more efficient than protons in creating upsets. Predictions using the two-parameters model are presented and discussed.**

***Index Terms*—Pions, prediction, protons, upsets.**

I. Introduction

OVER the last ten years, single-event effects have become a concern for the avionics systems [1]–[3]. Important work was done in the early 1990s that established the relation between error rates and altitude and latitude levels of aircrafts [4]. From this study, it was obvious that neutrons are the most important contribution for single-event upset (SEU).

These particles originate from the cosmic-ray cascades in the atmosphere. They are created when primary particles (mostly high-energy protons—galactic particles, solar wind) hit atmospheric atoms, resulting in a shower of secondaries (also called "cascade particles"). The cascades contain neutrons (nucleons) but also muons, pions, electrons, and photons. Among these particles, only neutrons and pions can cause major failures in VLSI.

In fact, it could be anticipated that the important decrease of the critical charge associated to a basic memory cell as the increasing integration of modern random-access memories (RAMs) poses the problem of their sensitivity to pions. Moreover, recent works have shown that due to the specific interaction mode involved in the pion$^+$–Si interactions (absorption mechanism, resonant enhancement of reaction cross-sections), the effectiveness of pions in inducing upset in dynamic RAM (DRAM) elements could be significant compared to that for proton and neutrons [5], [6]. Therefore, at aircraft altitude, where the pions exist in sufficient quantities, they could contribute greatly to the total event rates.

Little data exists in the literature [5]–[8] on devices' response to pion beams. In this paper, results of pion irradiations realized at the Gatchina facility are presented for a large set of static RAM (SRAM) and DRAM representing the technological evolution over these last ten years.

Manuscript received July 17, 2001.

S. Duzellier and D. Falguère are with ONERA-DESP, 31055 Toulouse, France (e-mail: duzellier@onecert.fr).

M. Tverskoy and E. Ivanov are with the PNP Insitute, Gatchina, Leningrad District, Russia (e-mail: tverskoy@mail.pnpi.spb.ru).

R. Dufayel and M.-C. Calvet are with EADS Launch Vehicles, F-78133 Les Mureaux Cedex, France (e-mail: richard.dufayel@lanceurs.aeromatra.com).

Publisher Item Identifier S 0018-9499(01)10677-5.

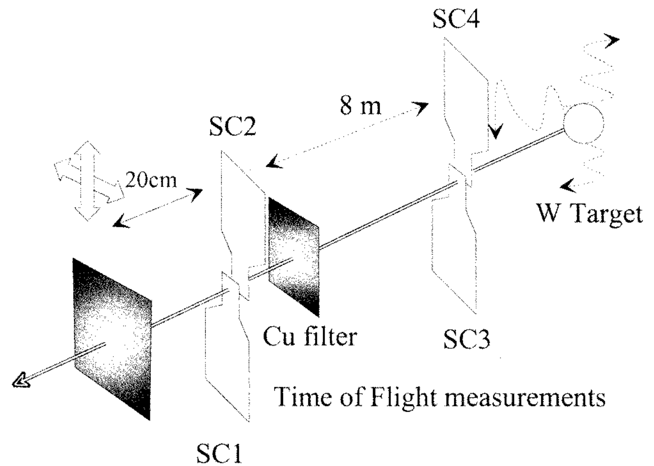

Fig. 1. Pion line setup (dosimetry and test board).

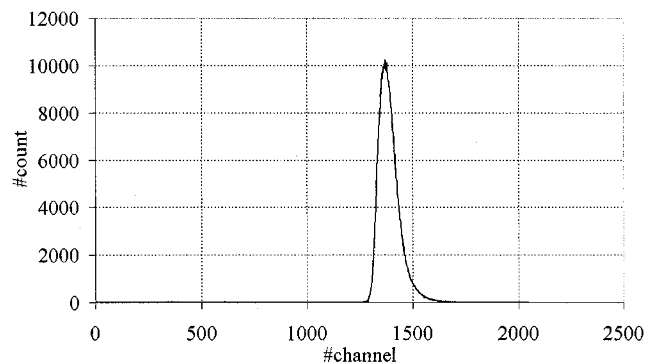

Fig. 2. Time-of-flight spectrum for the 147-MeV π^+ beam.

II. Test Conditions

Tests have been carried out on the accelerator facility at Gatchina (PNPI) [9]. The installation provides a primary 1-GeV proton beam directed toward Tungsten target. Pions are available as secondary beams. Beam monitoring was made using standard nuclear physics instruments such as scintillation counters and ionization chambers (Fig. 1).

Energy spectra of the beams are available (time-of-flight measurements, Fig. 2) and show a sharp spectrum with minimum (6%) contamination of electrons (positrons) and muons. A copper filter is placed before the counting system to absorb protons of the same momentum.

Three π^+ beams were used for the tests: 237, 147, and 58 MeV. The beam profile was measured using ionization

0018–9499/01$10.00 © 2001 IEEE

TABLE I
DEVICE TYPES AND TECHNOLOGICAL DATA

Device	Type	Process	Manufacturer
		SRAMs	
HM65756	256k	/	Temic
CY7C199	256k	0.8μm	Cypress
MT5C2568	256k	high speed/low power CMOS, 4T cell, double metal/poly layers	Micron
MT5C1008	1M	high speed/low power CMOS, 0.8 μm bulk, 4T cell, double metal/poly layers	Micron
TC551001	1M	/	Toshiba
KM681000	1M	0.5 μm, advanced CMOS technology	Samsung
M5M51008	1M	high performance CMOS, triple poly layer, R-load NMOS cell	Mitsubishi
HM65608	1M	0.6μm	Atmel
HM628512	4M	0.5μm Hi-CMOS, stacked PMOS lead transistor	Hitachi
		DRAMs	
SMJ416400	16M	0.5μm, trench capacitor	T.I.
EDI441024	4M	/	EDI
50G6269	64M	0.35μm, trench capacitor	IBM

chambers (Gaussian shape) and the spot size is 3 cm in diameter. The counting uses plastic scintillators in size bigger than the device. Then a correction factor is applied to the particle count to get the effective fluence seen by the chip. The irradiations were performed with normal incident beams and fluxes ranging from 3 to 8.10^5 particles/cm^2 .s. The parts were irradiated lid-on.

Because of this "low" flux, the time needed to perform an irradiation run is long (on the order of 1/2–1 h). However, at least 20 upsets were detected for each part to limit the statistical uncertainties of measured cross-sections.

The components tested were a set of SRAMs and DRAMs (see Table I) previously fully characterized with protons (and heavy ions) [10]–[15]. Some of them were parts from the flight lot of the EXEQ test bench (MIR Space Station [15]) or the SPICA/ICARE experiment (also onboard the MIR Station and SAC-C Argentinean satellite). When available, process details are given.

The components are scrubbed under exposure with the memory plan filled with a checkerboard pattern and the bias level is 5 V, save for the DRAM 64 Mbits from IBM (3.3 V). Only one or two devices per types were irradiated. In order to compare pion and proton data, we chose devices from the same date code as those that have been characterized with protons. Sometimes, because we had a limited number of components, the same parts irradiated at PNPI have also experienced several irradiations (high-energy heavy ions or/and protons).

III. EXPERIMENTAL RESULTS

The results are presented in Figs. 3–5. Pion measurements are compared with proton data obtained for the same parts or date code.

The Y-error bars are shown for the pion measurements because of the "low" statistics of events (related to the "low" flux available). No multiple-bit upsets were detected.

As shown in the figures, two main features exist for the pion curves.

1) For most of the devices tested (save for the M5M51008 and the 50G6269) and over the energy range used, the cross-section increases showing a plateau or a linear feature with energy. The greatest value is for the 237-MeV measurement,
2) Only two devices, the M5M51008 1-Mbit SRAM and the 50G6269 64-Mbit DRAM in a lower extent, exhibit a slight ≪bump≫ near E ≈ 150 MeV in their π^+ sensitivity curves.

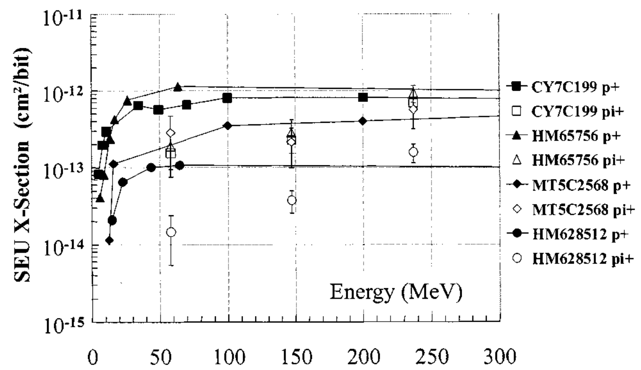

Fig. 3. Pion/proton data for the 256-K and 4-Mbit SRAMs.

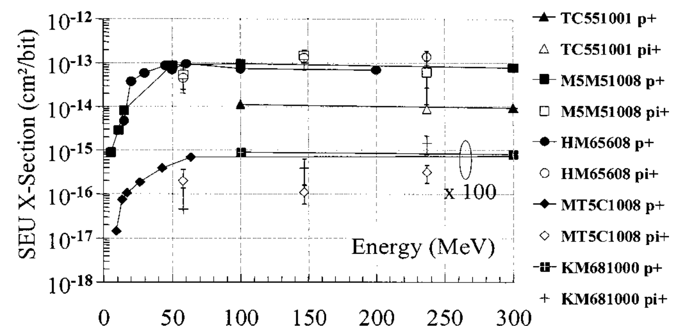

Fig. 4. Pion/proton data for the 1-Mbit SRAM's. Cross-sections for the MT5C1008 and KM681 000 have been divided by 100 to improve the readability of the graph.

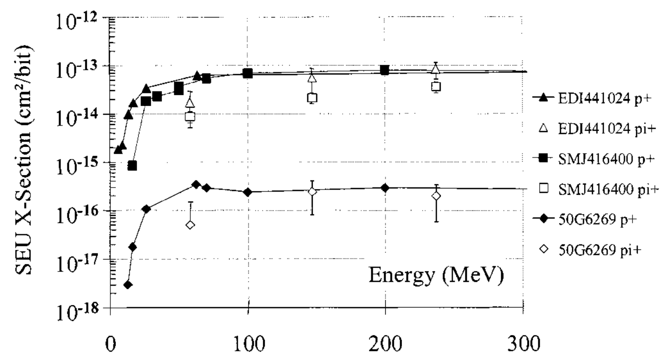

Fig. 5. Pion/proton data for all the DRAM devices.

As reported in point 1), the features of the device sensitivity and reaction cross-sections are not similar and the sensitivity resonance expected is not observed (it should be centered on nearly 150 MeV). As a matter of fact, the hypothesis of an electronic energy loss that would be at the origin of the events cannot be supported regarding the very low linear energy transfer of the pions for the energy range used (about 10^{-3} MeV/mg-cm^2). Therefore, it is clear that nuclear reactions with Si nucleus is the dominant mechanism.

From point 2), it seems that the energy dependence of the SEU cross-section behaves similarly to the reaction and absorption cross-sections for π–Si interactions. The SEU cross-section reflects merely the pion enhancement in the reaction cross section. But it is not demonstrated that pions are more effective than protons in creating upsets. Moreover, for the two devices with which we are concerned, pion and proton measurements lie within the statistical error. From these observations, it may be concluded that the absorption mechanism at resonance does not dominate at inducing upsets for these devices.

Concerning the relative effectiveness at inducing soft errors, at first we consider the 1-Mbit SRAM case. Mainly two different behaviors are observed. The Mitsubishi and Toshiba pion data lie close to the proton measurements (within a factor of two). The pion measurements at 237 MeV for the Samsung and Micron devices fit quite well the proton cross-section, but the straight-line feature of the characteristic leads to a much lower sensitivity of the devices with pions for 147 and 58 MeV.

The pion and proton cross-sections are compared on Figs. 6–8 (the line indicates equal cross-sections for both pions and protons). To make these comparisons, proton cross-sections at the three pions' energies were extrapolated from the proton sensitivity curves. For the 237- and 147-MeV measurements, the saturation part of the curve is reached; therefore the data points can be directly compared with saturation cross-section. The 58-MeV points are compared to the closer data (62 MeV) or to the average sensitivity calculated from surrounding energies (in the 40–60 MeV range).

For all of the devices, the greater cross-section measured with pions (for the range of energy used) is of the same order of magnitude as the one measured with protons. The maximum σ value is generally observed for E = 237 MeV (see Fig. 6).

For the lower energies (147 then 58 MeV), the protons are always more efficient at inducing errors (see Figs. 7 and 8).

Considering the DRAMs, Hoffman in [5] has observed a better ≪efficiency≫ for pions to create upsets across the 50–300 MeV range. For example, it was shown that for a set of 16- and 64-Mbit memories, the cross-section for 150-MeV pions is larger than those with protons by a mean factor of three except for two devices: one 16-Mbit and one 64-Mbit device. Both parts used a trench internal capacity technology, and in both cases they were the most robust parts.

In the framework of this study, for the three DRAM components tested and whichever the energy, pion and proton cross-sections do not differ strongly and proton cross-sections are always slightly greater than pion ones.

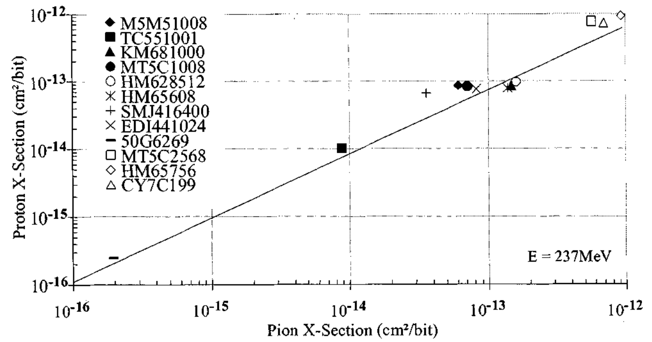

Fig. 6. Comparison of pion and proton data at 237 MeV. The p+/pi+ sensitivity ratio ranges from 0.6 to 1.9.

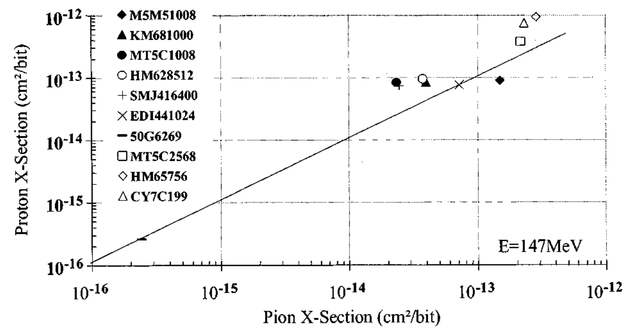

Fig. 7. Comparison of pion and proton data at 147 MeV. The p+/pi+ sensitivity ratio ranges from 0.6 to 3.6.

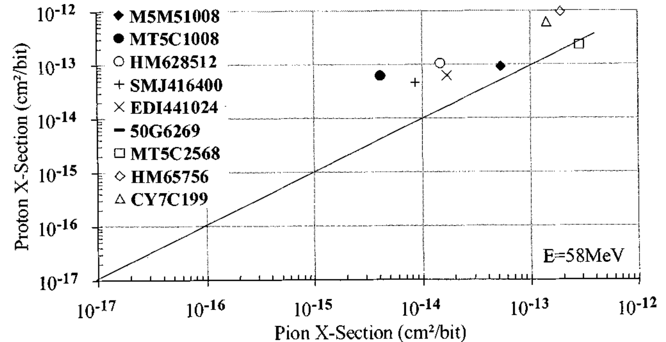

Fig. 8. Comparison of pion and proton data at 58 MeV. The p+/pi+ sensitivity ratio ranges from 0.8 to 15.

IV. Prediction of the Pion SEU Cross-Sections

We tried to calculate the pion cross-sections using the approach described in [16]. The two-parameters model (TPM) was originally developed to predict proton SEU cross-section. This method is based on the assumption that energy deposition from nuclear fragments in the sensitive volume (SV) is the main reason for upsets.

The two parameters used for the calculation are the sensitive volume V and the threshold energy E_{thr}. These parameters are determined from at least two experimental proton cross-sections (e.g., at different energies). So the volume where reactions occur (secondaries generation) is taken equal to the sensitive volume of the device. In practice, it is suitable to use the linear dimension d of the sensitive volume ($V^{1/3}$).

Then, the error rate is calculated from the following equation:

$$\sigma_{\text{seu}} = \sigma_{\text{in}}.n.V.\varepsilon\left(E_{\text{thr}}\right) \tag{1}$$

where $\varepsilon\left(E_{\text{thr}}\right)$ represents the proportion of nuclear reactions that actually leads to an event, n is the number of Si nuclei in 1 cm^3 ($n = 5.10^{22}$ for Si), and σ_{in} is the p+–Si inelastic cross-section. In a previous paper [17], it was shown that the results of the presented Monte Carlo code could be used for this calculation. The ability of this code to calculate the energy deposition in thin slabs of Si irradiated by protons was also demonstrated in [16].

TABLE II
PARAMETERS EXTRACTED FROM THE PROTON DATA FOR THE PION CALCULATIONS

Device type	Parameter d (μm)	E_{thr} (MeV)	Process
HM65756	8.8	3.55	/
CY7C199	4.65	1.7	0.8μm
MT5C2568	6.45	3.85	/
MT5C1008	3.25	3.45	0.8μm
TC551001	1.55	1.5	/
HM65608	3.25	2.9	0.6μm
KM681000	3.85	4.5	0.5μm
M5M51008	2.2	1.85	/
HM628512	2.45	1.75	0.5μm
SMJ416400	2.9	3.4	0.5μm
EDI441024	3.75	3.7	/

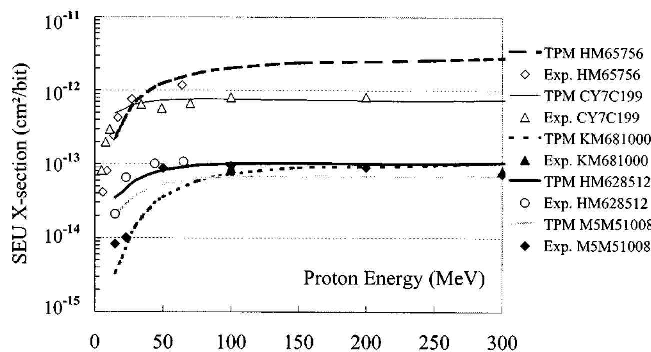

Fig. 9. Prediction of the proton cross-section using TPM for the CY7C199, HM65756, KM681000, M5M51008, and HM628 512 devices.

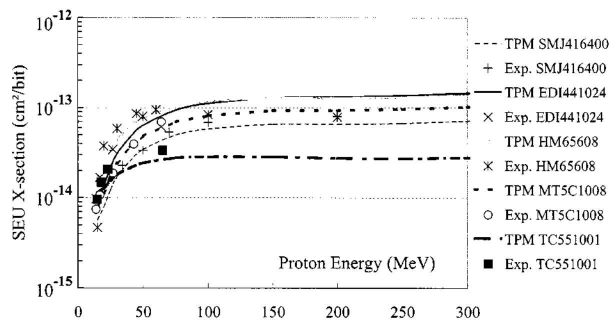

Fig. 10. Prediction of the proton cross-section using TPM for the HM65608, TC551001, MT5C1008, EDI441 024, and SMJ416 400 devices.

Parameters d and E_{thr} found for the set of devices in which we are interested are presented in Table II. Experimental data in the interval 15–1000 MeV of proton energies were used for analysis. These values are obtained from the best fit for the prediction of proton error rates (Figs. 9 and 10).

When compared with the process length parameter λ, one can see that as λ decreases, d and E_{thr} also tend slightly to lower values.

As one can see, in every case and for the 20–300 MeV energy range, the cross-section at saturation and the threshold are predicted with reasonable accuracy. At the same time, it seems that TPM tends to overestimate the SEU cross-section slightly at higher energies.

For the 64-Mbit DRAM 50G6269, we were not able to estimate TPM parameters. The experimental SEU cross-sections were very low, providing d of less than 1 μm. That quantity was determined as the lower limit of the model validity [17].

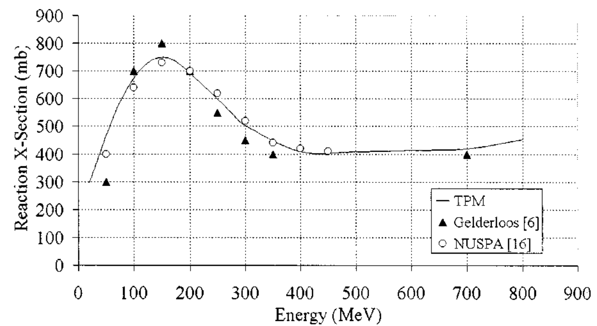

Fig. 11. Inelastic π^+–Si cross-sections. The TPM data are compared to Gelderloos [6] and NUSPA calculations [18].

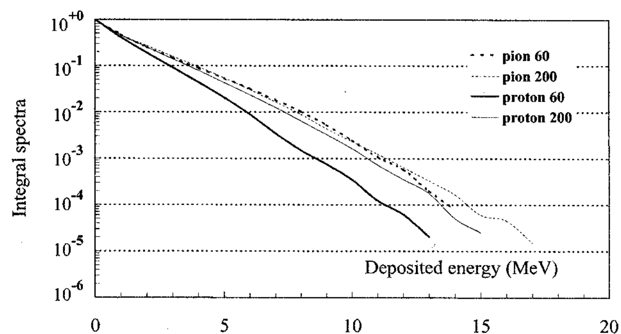

Fig. 12. Integral spectra of energy deposited in the M5M51008 sensitive volume ($d = 2.2$ μm).

Inelastic π^+–Si cross-sections calculated by our code are presented in Fig. 11 along with other results [5], [18]. Gelderloos *et al.* [6] showed that their calculated curve fits some of the existing experimental pion-nuclei inelastic cross-sections. This fact supports the use of an actual variant of the Monte Carlo code for the SEU cross-section analysis.

For calculation of pion interactions, we used the same code as in [16] and [17]. This code deals with elastic and inelastic modes in nucleon–nucleon and pion–nucleon interactions. The absorption of pions by nucleon pairs in nucleus is included. The cross-sections for the different mechanisms were taken as for free particles.

The first (cascade) stage of the reaction provides the fastest products including pions. They could be absorbed by a nucleon pair inside the nucleus or leave it. Then less energetic particles, including nuclear fragments, escape from the excited nucleus.

On the next stage of the calculation, we trace the "fate" of the particle in the volume V where charged particles deposit part of their energy. The probability of secondary interactions of fast particles with Si nuclei is calculated (for protons, neutrons, and pions). The contribution of all charged secondaries is taken into account in the calculation of the deposited energy in volume V. Usually 10^6 interactions are modeled to obtain the E_{dep} distribution. Analysis of this spectrum provides the factor $\varepsilon(E_{\mathrm{thr}})$, and so the SEU cross-sections can be calculated for different projectiles. For example, Fig. 12 presents integral spectra of the energy deposited in the cell of the M5M51008 ($d = 2.2$ μm) for 60 and 200 MeV pion/proton irradiations.

The two pion spectra are very closed, but the proton spectra are quite different for the two energies chosen. This reflects the

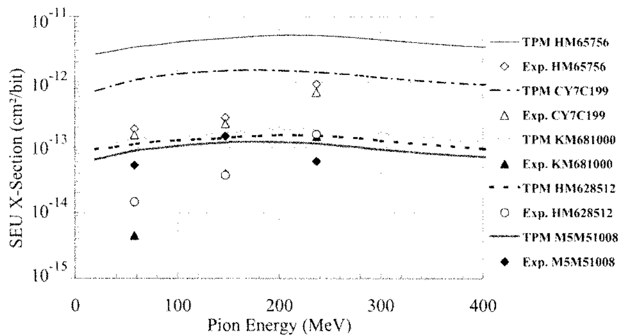

Fig. 13. TPM cross-section for π^+ compared to the experimental data for HM65756, CY7C199, KM681000, HM628 512, and M5M51008.

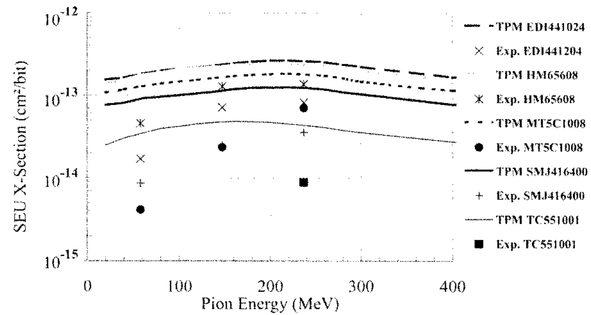

Fig. 14. TPM cross-section for π^+ compared to the experimental data for SMJ416400, EDI441024, HM65608, MT5C1008, and TC551 001.

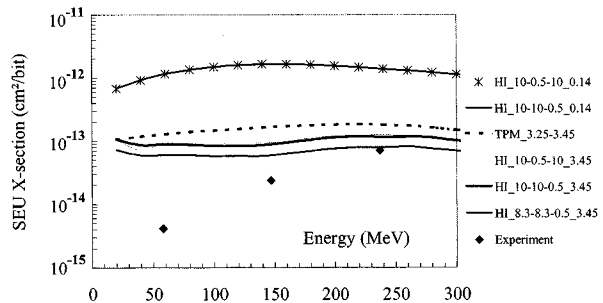

Fig. 15. Comparison of experimental and calculated pion cross-sections for the MT5C1008. Standard TPM data are compared with TPM results obtained with parameters deduced from heavy-ion experiments.

fact that there is no pion production in proton collisions at 60 MeV, but it can occur at 200 MeV.

The absorption of pion by nucleon pair provides two additional fast nucleons (with total energy about 140 MeV) inside nuclei. These nucleons are the origin of a new cascade process, making the picture of interaction more complicated. This fact is reflected in the slopes of the curves presented in Fig. 14.

Figs. 13 and 14 present the calculated curves using TPM along with experimental data.

The best agreement between experimental and calculated results was obtained for the 1-Mbit SRAM M5M51008. For the other parts, the 237-MeV experimental SEU cross-section can be predicted within a factor of 2–3, but the calculations do not fit the measurements at low energies. For the latter, the predictions greatly overestimate the experimental results.

Considering the most integrated devices, as the sensitive volume associated is very small, it is obvious that the validity of the method is doubtful. In fact, additional analysis was made for two parts (the MT5C1008 and HM628 512 devices) to determine whether the assumption of the cubic feature of the sensitive volume is valid and whether the $E_{\rm thr}$ parameter values are also consistent with the technology used. As a matter of fact, the SV lateral dimensions can be deduced for the heavy-ion (HI) cross-section at saturation. Moreover, the sensitive depth as well as the critical energy can be determined from other methods. For some devices tested, d and $E_{\rm thr}$ values have been proposed [19].

In Fig. 15, we present detailed results for the MT5C1008 obtained from additional calculations. Three cases are shown and compared to the TPM results previously presented in Fig. 14.

1) Dimensions of the sensitive volume and the threshold energy are estimated from HI data. The lateral dimensions[1] $a = c = 10\ \mu$m, the thickness[2] $d = 0.5\,\mu$m, and $E_{\rm thr} = 0.14$ MeV. Calculations are made for two "directions of the pion beam" normal incidence (10–10–0.5) or grazing incidence (10–0.5–10). To model these two directions, the depth is alternately considered as a lateral or vertical dimension (the volume remains the same).
2) The SV dimensions are the same as previously but the $E_{\rm thr}$ parameter is taken from the proton data ($E_{\rm thr} =$ 3.45 MeV). Calculations for two "directions of the pion beam" are also performed.
3) Here we use the volume determined by TPM for that part but take the thickness from HI measurements. Therefore, $a = c = 8.3\mu$m, $d = 0.5\,\mu$m, and $E_{\rm thr} = 3.45$ MeV.

It can be seen that the incidence direction has no influence on the result; therefore the shape, cubic, or parallelepiped rectangle of the volume is not important for the calculation.

At the opposite, the $E_{\rm thr}$ value strongly affects the result of the calculation. A decade of difference is observed and a much greater overestimation obtained with $E_{\rm thr} = 0.14$.

As a matter of fact, the set of parameters that gives the best results is $a = c = 8.3\,\mu$m, $d = 0.5\,\mu$m, and $E_{\rm thr} = 3.45$. But in any case, the 58- and 147-MeV measurements are badly predicted. We have no clear explanation about these large discrepancies. Considering possible uncertainties on the experimental measurements, the fluence of pions was in the interval where scintillations counters have efficiency near 100%. Moreover, the error in positioning the chip would result in a lower receive fluence and therefore a higher cross-section.

At least considering the calculations, the prediction of proton SEU cross-section gives results with sufficiently good accuracy. Moreover, we have seen that the inelastic pion cross-section is correctly described. Therefore, one can conclude that the code successfully treats the main features of inelastic nuclear cascades. The possible mechanism that is not taken into account is the absorption of pions by nuclear structure more complex than two nucleons. Such processes could provide additional fragments depositing energy in the volume V. On the other hand, it seems reasonable to suppose that the probability of pion absorption by three or more nucleons is much less than by two.

[1]Lateral dimensions were calculated from the saturation cross-section.

[2]The sensitive thickness and threshold energy are deduced from the "deconvolution" method [17].

Additional experiments including measurements of the energy deposited in thin Si slabs irradiated by pions would help to shed light on this problem.

V. Conclusions

Experimental π^+-induced SEU cross-sections for a large set of modern memories were measured at the Gatchina facility for 58-, 147-, and 247-MeV beams. Obtained results show that, save for two devices, the cross-section increases as a function of the pion energy in the investigated interval.

For the range of energy used, the greater cross-section measured with pions is the same order of magnitude as the proton sensitivity at saturation. The maximum σ value is generally observed for $E = 237$ MeV, and for the set of tested devices, it is not demonstrated that pions are more effective than protons in creating upsets.

From the sensitivity curves, it is clear that nuclear reaction with Si nucleus is the dominant mechanism, but the SEU cross-section rarely reflects the pion enhancement in the reaction cross-section. From these observations, it may be concluded that the absorption mechanism at resonance does not dominate at inducing upsets for these devices.

The two-parameter model has been applied for calculating the pion SEU cross-sections. It has been demonstrated that the shape—cubic or parallelepiped rectangle—of the volume is not important for the calculation. The sensitive depth and critical energy seem to drive the results of the calculations.

The results at "low" energies (58 and 147 MeV) generally overestimate the experimental data while the 237-MeV cross-section can be predicted within a 2–3 factor.

References

[1] E. Normand, "Single-event effects in avionics," *IEEE Trans. Nucl. Sci.*, vol. 43, p. 461, Apr. 1996.

[2] J. F. Ziegler, "Terrestrial cosmic rays," *J. Res. Develop. IBM*, vol. 40, no. 1, p. 19, Jan. 1996.

[3] C. S. Dyer, A. J. Sims, J. Farren, and J. Stephen, "Measurements of the SEU environment in the upper atmosphere," *IEEE Trans. Nucl. Sci.*, vol. 36, no. 6, p. 2275, 1989.

[4] E. Normand and T. J. Baker, "Altitude and latitude variations in avionics SEU and atmospheric neutron flux," *IEEE Trans. Nucl. Sci.*, vol. 40, p. 1484, 1993.

[5] G. J. Hoffman, R. J. Peterson, C. J. Gelderloos, R. A. Ristinen, M. E. Nelson, A. Thompson, J. F. Ziegler, and H. Mullfeld, "Light-hadron induced SER and scaling relations for 16 and 64 Mb drams," *IEEE Trans. Nucl. Sci.*, vol. 47, p. 403, Apr. 2000.

[6] C. J. Gelderloos *et al.*, "Pion-induced soft upsets in 16 Mbit DRAM chips," *IEEE Trans. Nucl. Sci.*, vol. 44, p. 2237, Dec. 1997.

[7] J. F. Dicello, C. W. McCabe, J. D. Doss, and M. Paciotti, "The relative efficiency of soft-error induction in 4K static RAM's by muons and pions," *IEEE Trans. Nucl. Sci.*, vol. NS-30, no. 6, p. 4613, 1983.

[8] J. F. Dicello, M. E. Schillaci, C. W. McCabe, J. D. Doss, M. Paciotti, and P. Berardo, "Meson interactions in NMOS and CMOS static RAMs," *IEEE Trans. Nucl. Sci.*, vol. NS-32, no. 6, p. 4201, 1985.

[9] N. K. Abrossimov, K. N. Ermakov, E. M. Ivanov, V. M. Lebedev, Y. T. Mironov, V. V. Pashuk, G. A. Riabov, V. M. Smolin, M. G. Tverskoy, and S. Duzellier, "The potential of the radiation effects investigations on the accelerator facilities at Gatchina," in *Proc. 5th RADECS Conf.*, 1999, p. 159.

[10] P. Calvel, P. Lamothe, C. Barillot, S. Duzellier, and R. Ecoffet, "Space radiation evaluation of 16Mbits DRAM's for mass memory applications," *IEEE Trans. Nucl. Sci.*, vol. 41, no. 6, p. 2267, 1994.

[11] S. Duzellier, D. Falguère, and R. Ecoffet, "Heavy ion/proton test results on high integrated memories," in *IEEE Radiation Effects Data Workshop Rec.*, 1993, p. 36.

[12] D. Falguère, S. Duzellier, and R. Ecoffet, "SEE in-flight measurement on the MIR orbital station," *IEEE Trans. Nucl. Sci.*, vol. 41, no. 6, p. 2346, 1994.

[13] S. Duzellier, D. Falguère, R. Ecoffet, and I. Tsourilo, "EXEQ II et EXEQ III: expérience embarquées pour l'étude des événements singuliers," in *Proc. RADECS97*, 1997, p. 504.

[14] S. Duzellier, R. Ecoffet, D. Falguère, T. Nuns, L. Guibert, W. Hajdas, and M.-C. Calvet, "Low energy proton induced SEE in memories," *IEEE Trans. Nucl. Sci.*, vol. 44, no. 6, p. 2306, 1997.

[15] D. Falguère, S. Duzellier, R. Ecoffet, and I. Tsourilo, "EXEQ I–IV: SEE in-flight measurement on the MIR orbital station," in *IEEE Radiation Effects Data Workshop Rec.*, 2000, p. 89.

[16] V. V. Miroshkin and M. G. Tverskoy, "Two parameter model for predicting SEU rate," *IEEE Trans. Nucl. Sci.*, vol. 41, no. 6, pp. 2085–2092, 1994.

[17] ——, "A simple approach to SEU cross section evaluation," *IEEE Trans. Nucl. Sci.*, vol. 45, no. 6, p. 2884, 1998.

[18] H. H. K. Tang, "Nuclear physics of cosmic ray interaction with semiconductor materials: Particle-induced soft errors from physicist's perspective," *J. Res. Develop. IBM*, vol. 40, no. 1, p. 91, Jan. 1996.

[19] C. Inguimbert, S. Duzellier, R. Ecoffet, L. Guibert, J. Bark, and M. Chabot, "Using a carbon beam as probe to extract the thickness of sensitive volumes," in *Proc. 5th RADECS Conf.*, 1999, p. 180.